Radiophysics and Quantum Electronics, Vol. 41, No. 10, 1998

A THEORY OF OPTICAL COHERENCE TOMOGRAPHY

L. S. Dolin

UDC 535.36

Analytical models of optical coherence tomography (OCT) of strongly turbid media of the type of biological tissues are developed on the basis of the theory of wave scattering in random inhomogeneous media. Similarity relations for signals of coherent and pulsed sounding are established, and general expressions for random realizations and statistical characteristics of tomograms are obtained. It is shown that after the appropriate modification the theory of image transfer in turbid media can be used for analysis of their informative properties. Simple formulas for estimating the visibility depth into the internal structure of biological tissues are proposed.

1. INTRODUCTION

The development of the methods of optical diagnostics of human body tissues and organs in the therapeutic transmittance window (0.6 to 1.3 μm) has approached the stage of their practical implementation and the creation of medical instruments [1]. The most impressive progress [2–5] was made in the optical coherence tomography (OCT), i.e., the formation of images of the internal structure of biological tissues using a lidar based on a continuous radiation source with femtosecond coherence times and a Michelson interferometer in whose object arm the observation object is placed. In this case, reflections from the tissue layers with thickness of the order of half the length of the coherent trains comprising the continuous illumination beam are observed separately. The light signals of the OCT system are emitted and received by the end of the single-mode light fiber, which is projected onto the studied region of tissue with the help of an optical system. Therefore, the confocal observation pattern is realized, allowing us to obtain a certain gain in the angular resolution.

The holographic and interferometric methods of the layer-by-layer visualization of the internal structure of scattering objects [6] has long since been studied (H. S. Caufield, 1968; A. P. Ivanov, I. M. Gurskii, A. P. Chaikovskii, A. A. Kumeisha, and V. N. Shcherbakov, 1976–1981; I. L. Katsev, 1985). Although the theoretical models of the OCT have not been developed in detail, one can find some interesting publications in this field [7, 8]. In this paper, we attempt to answer two questions: 1. To which extent and in what way can the results of the theory of instrumented vision in turbid media [6, 9] that refer to the observation systems with direct photodetection of the signal be used for solving the problems of OCT? 2. What are the specific features of the OCT methods and how can they be allowed for when developing models of tomographic images?

To make the presentation of the material more perspicuous (and, at the same time, introduce the necessary terms and notations), in Sections 2.2 and 4 we give a schematic description of the process of formation of informative and noise video signals in the heterodyne receiver of the OCT system. A

Institute of Applied Physics of the Russian Academy of Sciences, Nizhny Novgorod, Russia. Translated from Izvestiya Vysshikh Uchebnykh Zavedenii, Radiofizika, Vol.41, No.10, pp. 1258–1289, October 1998. Original article submitted March 30, 1998.

 0033-8443/98/4110-0850$20.00

more in-depth study of these problems is proposed in [10], which was written under the guidance of V. M. Gelikonov.

2. FORMULATION OF THE PROBLEM

2.1. Model of the medium

As an optical model of the observation object, we consider a medium with random inhomogeneous distribution of complex permittivity

$$\varepsilon(\vec{r}) = \langle\varepsilon\rangle[1 + \varepsilon_1(\vec{r}) + \varepsilon_2(\vec{r})]. \tag{1}$$

Its average value $\langle\varepsilon\rangle$ is assumed to be constant, the term ε_1 describes the fluctuations of ε with spatial scale $l_1 \gg \lambda$, and ε_2 are the fluctuations with scale $l_2 < \lambda$. The distributions $\varepsilon_{1,2}(\vec{r})$ form the locally homogeneous isotropic random fields with the space-correlation functions

$$B_{\varepsilon_{1,2}}(\vec{r},\rho) = \left\langle \varepsilon_{1,2}(\vec{r}+\vec{\rho}/2)\varepsilon^*_{1,2}(\vec{r}-\vec{\rho}/2)\right\rangle \tag{2}$$

and the space spectra

$$\Phi_{1,2}(\vec{r},\kappa) = (2\pi)^{-3}\iiint\limits_{-\infty}^{\infty} B_{\varepsilon_{1,2}}(\vec{r},\rho)\mathrm{e}^{-i\vec{\kappa}\vec{\rho}}d^3\vec{\rho}, \quad \kappa = |\vec{\kappa}|. \tag{3}$$

The fluctuations of ε are assumed to be small ($B_{\varepsilon_{1,2}}(\vec{r},0) \ll 1$).

It is also assumed that along with the continuously distributed inhomogeneities in the medium there exist some local scatterers the distance between which exceeds the size of the resolution element of a lidar. These inhomogeneities are characterized by their differential scattering cross section Σ_{diff} or effective scattering area $\text{ESA} = 4\pi\Sigma_{\text{diff}}$.

2.2. The process of image formation

In the OCT system, the separate observation of reflections from tissue elements that are located at different depths (z) is performed by measuring the cross-correlation function of the reflected signal and the reference signal that is a copy of the sounding signal (as in the case of matched reception of complex signals). The reference signal is formed by branching the source light to the reference arm of the light- fiber Michelson interferometer. The scattered and reference waves are added on the receiver photodetector. The tomographic signal is obtained as a result of the detection of Doppler beats, which emerge in the photodetector current in response to variation of the length of the interferometer reference arm. The image in the plane $z = \text{const}$ is formed due to the shift of the transceiving aperture of the lidar along the tissue surface (Fig. 1).

The end of the fiber-optical single-mode waveguide is assumed to be the aperture (the presence of the focusing system between the aperture and the tissue will be allowed for later). The emitted (u_0) and received (u_S) fields inside the waveguide (between its end and the signal splitter) are written as

$$u_{0,S}(\vec{r}_\perp, z, t) = M(\vec{r}_\perp)\, v_{0,S}(t \mp z/c), \tag{4}$$

where $\vec{r}_\perp$ is the radius vector of a point in the waveguide cross section Σ_w, z is the coordinate along its axis, c is the phase velocity of the wave, the function M characterizes the transverse structure of the mode and satisfies the normalization condition

$$\int\limits_{\Sigma_w} M^2 d^2\vec{r}_\perp = 1, \tag{5}$$

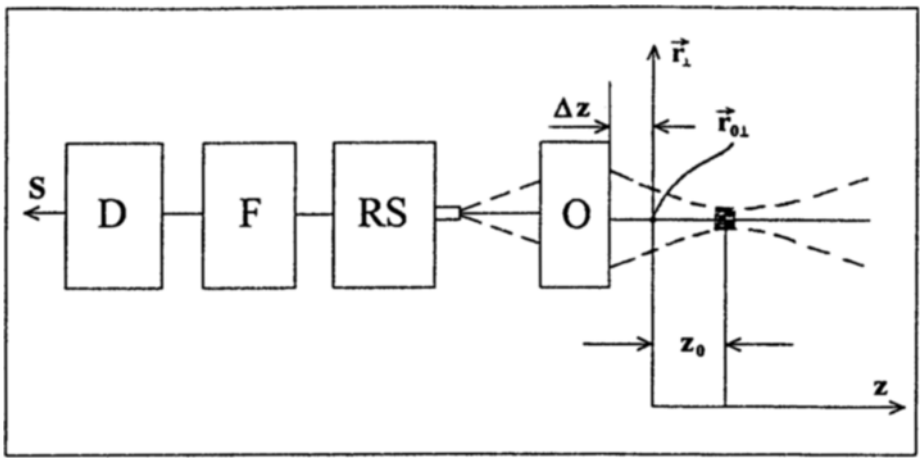

Fig. 1. OCT flow chart. O is the optical system of the illumination-beam formation, RS is the radiation source and heterodyne photoreceiver with units for delay of the reference signal and transverse scanning, F is the band-pass filter with amplifier, D is the videosignal detector, and $\vec{r}_{0\perp}$ and z_0 are the coordinates of the detected tissue element.

v_0 is the stationary normal quasimonochromatic process with zero mean $\overline{v_0} = 0$, center frequency ω_0, and the autocorrelation function

$$B_0(\tau) = \overline{v_0(t+\tau)\, v_0(t)} = P_0\, b_0(\tau)\, \cos\omega_0\tau, \tag{6}$$

P_0 is the average power of the emitted signal, $b_0(0) = 1$, and the bar denotes averaging over the realization ensemble of the random process v_0.* This process is also characterized by the energy spectrum

$$S_0(\omega) = \frac{1}{2\pi}\int\limits_{-\infty}^{\infty} B_0(\tau)\, \cos\omega\tau\, d\tau. \tag{7}$$

The time scale of the process correlation τ_c (coherence time) and the characteristic width of its energy spectrum Δf_0 are determined by the expressions

$$\tau_c = \int\limits_{-\infty}^{\infty} b_0^2(\tau)\, d\tau, \quad \Delta f_0 = 1/\tau_c. \tag{8a, b}$$

Assuming that the interferometer splitter is symmetric (half of the power of the incident light beam is branched off to the adjacent arm), we write the fields of the received (u_S) and reference (u_r) signals on the receiver photodetector in the form

$$u_S = \frac{1}{\sqrt{2}} M(\vec{r}_\perp) v_S(t), \quad u_r = \frac{1}{\sqrt{n}} M(\vec{r}_\perp) v_0(t - t_0),$$

$$n = P_0/P_r, \quad P_{0,r} = \int\limits_{\Sigma_w} \overline{u_{0,r}^2}\, d^2\vec{r}_\perp .$$

*Note that in accordance with Eqs. (4)–(6), u_0^2 can be considered to be an instantaneous value of the energy flux density.

Here n is the ratio between the average powers of the emitted (P_0) and reference (P_r) signals, and t_0 is the delay time of the reference signal with respect to the sounding signal; the delay, which is common for the signals v_0 and v_S and emerges as light is transported to the photodetector, is omitted.

At the detector output, the field $(u_r + u_S)$ creates the photocurrent

$$i = \eta \int_{\Sigma_w} \overline{\overline{(u_r + u_S)^2}}\, d^2\vec{r}_\perp + i_{sh} \cong \frac{\eta}{n}\overline{\overline{v_0^2}} + \eta\sqrt{\frac{2}{n}}\overline{\overline{v_S(t)\, v_0(t - t_0)}} + i_{sh}\,, \tag{9}$$

where η is the photodetector sensitivity [A/W], i_{sh} is the shot current, the double bar denotes the smoothing of short- period pulsations of the signal power due to the photodetector inertia; the term $\sim v_S^2$ on the right-hand side of Eq. (11) is rejected in accordance with the condition $v_S \ll v_0$.

The first term in Eq. (11) contains the constant component

$$i_r = \eta P_0/n \tag{10}$$

and the fluctuation component

$$i_{fl} = \eta\left(\overline{\overline{v_0^2}} - P_0\right)/n\,. \tag{11}$$

The second term also has the noise component; however, for $v_S \ll v_0$ it is small compared with i_{fl}. Therefore, the final expression for i is approximately written as the sum of the constant (i_r), useful (i_u), and noise (i_n) currents

$$i = i_r + i_u + i_n\,, \tag{12}$$

assuming that

$$i_u = \eta\sqrt{2/n}\,\overline{v_S(t)\, v_0(t - t_0)}\,, \quad i_n = i_{sh} + i_{fl}. \tag{15a, b}$$

In the case of fixed time of the reference signal delay, the currents i_r and i_u are indistinguishable. However, as t_0 varies, the current i_u also becomes a function of time and can be separated from the average current of the reference signal (i_r) using the band-pass filter, which is also a means of noise suppression. Let us clarify it, using a simple example.

Let a point reflector located in a homogeneous medium at a distance z from the lidar be the observation object. Then $v_S(t) \sim v_0(t - 2z/c)$ and in accordance with Eq. (15a) and (6) $i_u \sim B_0(t_0 - 2z/c)$.

If in Eq. (6) we assume that

$$b_0(\tau) = \exp\left[-\frac{\pi}{2}\left(\frac{\tau}{\tau_c}\right)^2\right], \quad \omega_0 = 2\pi f_0\,, \tag{16}$$

and the delay time of the reference signal varies as $t_0 = \beta t$, then

$$\begin{gathered} i_u \sim P_0 \exp\left[-\left(\frac{\Delta t}{t_1}\right)^2\right]\cos(2\pi f_1 \cdot \Delta t), \\ \Delta t = t - 2z/(\beta c), \quad t_1 = \sqrt{\frac{2}{\pi}}\cdot\frac{\tau_c}{\beta}, \quad f_1 = \beta f_0\,. \end{gathered} \tag{17a - d}$$

As is obvious from Eq. (17), the useful signal $i_u(t)$ has the form of a pulse with carrier frequency f_1 and duration $2t_1$. The arrival time of its maximum is determined by the distance to the scatterer: $t_m = 2z/\beta c$. The spectrum of this pulse is a Gaussian curve with center frequency f_1 and width

$$\Delta f_1 = \beta\,\Delta f_0 = \beta/\tau_c\,, \tag{18}$$

such that the relative width of the pulse spectrum coincides with the relative width of the energy spectrum

of the source ($\Delta f_1/f_1 = \Delta f_0/f_0$).

Below, it is assumed that the signal i passes through the filter with passband $f_1 - \Delta f_1/2 < f < f_1 + \Delta f_1/2$ and is transformed into the signal $\Delta i = i_u + \Delta i_n$ (Δi_n is the noise current at the filter output), which goes to the linear or quadratic detector.* The image is formed by visualizing the video signal S_1 or S_2, which is taken from the linear or quadratic detector, as a function of the variable $z_0 = ct_0/2$ and coordinates of the point of intersection between the axis of the light beam and the boundary of the medium ($\vec{r}_{0\perp}$). To simplify the subsequent formulas, we use the dimensionless signals of the type

$$S_1(\vec{r}_{0\perp}, z_0) = \overline{\overline{|\Delta i|}} \Big/ i_r\sqrt{n} = S_{u_1} + S_{n_1}, \quad S_{u_1} = \overline{\overline{|i_u|}} \Big/ i_r\sqrt{n}, \tag{19a, b}$$

$$S_2(\vec{r}_{0\perp}, z_0) = \overline{\overline{(\Delta i)^2}} \Big/ i_r^2 n = S_{u_2} + S_{n_2}, \quad S_{u_2} = i_u^2/i_r^2 n, \tag{20a, b}$$

where the double bar denotes the smoothing of oscillations with frequency $2f_1$, $S_{u\,1,2}$ is the useful signal at the output of the linear or quadratic detector, and $S_{n\,1,2}$ is the noise signal. The signal $S_{1,2}(z_0)$ with fixed $\vec{r}_{0\perp}$ is called the image line, and the maximum value of z_0 is called the line length (z_l). As is obvious from the relations $z_0 = ct_0/2$ and $t_0 = \beta t$, the parameter β is expressed via the line length and its formation time (t_l) in the form

$$\beta = 2z_l/ct_l. \tag{21}$$

3. SIMILARITY RELATIONS FOR SIGNALS OF PULSED AND COHERENT OPTICAL SOUNDING

The signal v_S that results from light scattering by the "frozen" inhomogeneities of the permittivity of the medium is related to the sounding signal v_0 by the linear relation

$$v_S(\vec{r}_{0\perp}, t) = \int_0^\infty v_0(t - t')\, H(\vec{r}_{0\perp}, t')\, dt' \tag{22}$$

(previously, to simplify the formulas, the dependence of v_S on $\vec{r}_{0\perp}$ was not given explicitly).

In accordance with Eqs. (6), (15a), and (22), the useful current (i_u) from the photodetector of the OCT system is presented in terms of the function H (the pulsed response of the medium) in the form

$$i_u(\vec{r}_{0\perp}, t_0) = i_r\sqrt{2n} \int_0^\infty b_0(t_0 - t)\, \cos\omega_0(t_0 - t)\, H(\vec{r}_{0\perp}, t)\, dt, \tag{23}$$

and the useful signal at the output of a quadratic detector is determined by the relations

$$S_{u_2}(\vec{r}_{0\perp}, t_0) = \overline{\overline{i_u^2}} \Big/ i_r^2 n = (b_1^2 + b_2^2), \tag{24}$$

$$\left\{ \begin{array}{c} b_1 \\ b_2 \end{array} \right\} = \int_0^\infty b_0(t_0 - t)\, H(\vec{r}_{0\perp}, t) \left\{ \begin{array}{c} \cos\omega_0 t \\ \sin\omega_0 t \end{array} \right\} dt, \tag{25}$$

which result from Eqs. (20b) and (23).

Let us write the sounding signal in the form of the regular quasimonochromatic pulse

$$v_0(t) = A_0\, b_0(t)\, \cos\omega_0 t, \tag{26}$$

*In actual tomographic systems a more complicated detection is used. However, comparing the results of linear and quadratic detection, we already obtain sufficient information on the dependence of tomogram properties on the parameters of a videosignal detector.

which is similar to the autocorrelation function (6) of a continuous signal.

As is obvious from Eqs. (26) and (22), in this case the scattered signal $v_S(\vec{r}_{0\perp}, t)$ in the waveguide channel of the lidar repeats the dependence $i_u(\vec{r}_{0\perp}, t)$, and its power

$$P_S(\vec{r}_{0\perp}, t) = \overline{\overline{v_S^2}} = \frac{A_0^2}{2}\left[\left(b_1^2 + b_2^2\right)\right]_{t_0=t} \tag{27}$$

reproduces the dependence $S_{u_2}(t)$ (the double bar in Eq. (27) denotes the averaging of oscillations of the power with frequency $2\omega_0$).

Consequently, it turns out that if we know the energy response of the medium $P_S(\vec{r}_{0\perp}, t)$ to the pulsed signal with power

$$P_0(t) = \overline{\overline{v_0^2}} = P_0(0)\, b_0^2(t)\,, \tag{28}$$

then the signal S_{u_2} at the output of the OCT system with quadratic detector of video signal is determined from the relation

$$S_{u_2}(\vec{r}_{0\perp}, t_0) = p_S(\vec{r}_{0\perp}, t_0)\,, \tag{29}$$

where

$$p_S(\vec{r}_{0\perp}, t) = P_S(\vec{r}_{0\perp}, t)/\, P_0(0) \tag{30}$$

is the coefficient of signal transfer (the inverse of the attenuation coefficient of the power of a signal arriving from the medium in time t after the sounding pulse was sent (28)).

The useful signal taken from the linear detector is expressed in terms of p_S in the form

$$S_{u_1} = \frac{1}{\pi}\sqrt{8S_{u_2}} = \frac{1}{\pi}\sqrt{8p_S}. \tag{31}$$

Therefore, in the OCT system, after the correlation processing of a continuous scattered signal one can observe the formation of a copy of the signal formed at the output of an ideal energy receiver (with the passband $\Delta f > 1/\tau_c$) in the case of sounding of the medium by a light pulse with power (28). The pulsed response of the medium is reproduced by a correlation meter as a function of the delay time (t_0) of the reference signal. Therefore, to determine the distance to the scatterer (z), we can use the relation $z = ct_0/2$. The pulse duration (28)

$$\tau_p = \int_{-\infty}^{\infty} P_0(t)\, dt \Big/ P_0(0) \tag{32}$$

is equal to the coherence time of the continuous signal ($\tau_p = \tau_c$). Therefore, in the case of continuous sounding, the size of the resolution element with respect to distance (Δz_e) is related to the coherence time of the field (τ_c) by the relation $\Delta z_e = c\tau_c/2$.

4. INTERNAL NOISES IN SYSTEMS OF COHERENT AND PULSED SOUNDING

An image formed by the system of coherent sounding has a random component, which is created by internal noises and fluctuations of the useful signal $S_{u_{1,2}}$. The latter are due to the random distortions of the light-wave field in the process of its propagation and the random structure of sounded inhomogeneities. Skipping the problem of fluctuations of the useful signal, let us first estimate the level of internal noises with respect to a statistically average useful signal $\langle S_{u_{1,2}} \rangle$, i.e., the signal averaged over the ensemble of realizations of the fields $\varepsilon_{1,2}$.

In accordance with Eq. (15), the noise current from the photodetector of the OCT system is equal to the sum of the shot current (i_{sh}) and the current i_{fl}, which reproduces the power fluctuations of the reference light beam (excess noise). At the output of the filter with passband $f_1 - \Delta f_1/2 < f < f_1 + \Delta f_1/2$

(see Eq. (18)), the dispersion of the shot current is

$$\overline{i_{\text{sh}}^2} = 2ei_{\text{r}}\Delta f_1 = 2ei_{\text{r}}\beta/\tau_{\text{c}}. \tag{33}$$

If the current i_{fl} is assumed to be a normal random process, then, ignoring the photodetector inertia, its autocorrelation function can be written in the form

$$B_{\text{fl}}(\tau) = \overline{i_{\text{fl}}(t+\tau)i_{\text{fl}}(t)} = i_{\text{r}}^2\, b_0^2(\tau) \tag{34}$$

in terms of the autocorrelation function of the sounding (reference) signal v_0. As is obvious from Eq. (34), the power spectrum of the signal i_{fl} has characteristic width $\sim\Delta f_0$, and its value at the zero frequency is determined from the expression

$$F_{\text{fl}} = 2\int_{-\infty}^{\infty} B_{\text{fl}}(\tau)\,d\tau = 2i_{\text{r}}^2\tau_{\text{c}}\,. \tag{35}$$

Therefore, for $f_1 \ll \Delta f_0$ the current dispersion i_{fl} at the output of the band-pass filter is

$$\overline{i_{\text{fl}}^2} = 2i_{\text{r}}^2\tau_{\text{c}}\,\Delta f_1 = 2\beta i_{\text{r}}^2. \tag{36}$$

The ratio between the average powers of the useful signal and noise at the filter output

$$(\text{S/N}) = \frac{\overline{\langle i_{\text{u}}^2\rangle}}{\overline{i_{\text{sh}}^2} + \overline{i_{\text{fl}}^2}} \tag{37}$$

with allowance for Eqs. (33) and (36) and relation $\overline{\langle i_{\text{u}}^2\rangle} = ni_{\text{r}}^2 p_S$ (see Eqs. (20b) and (29)) is written as

$$(\text{S/N}) = \frac{\chi\langle p_S\rangle}{\beta(1+\delta)}, \tag{38}$$

$$\chi = \eta P_0\tau_{\text{c}}/(2e), \quad \delta = \overline{i_{\text{fl}}^2}\Big/\overline{i_{\text{sh}}^2} = \frac{2}{n}\chi \quad (e = 1.6\cdot 10^{-19}\ \text{K}). \tag{39a, b}$$

If the signal $(i_{\text{u}} + \Delta i_{\text{n}})$ arrives at the quadratic detector (see Eq. (20a,b)), the signal-to-noise ratio with respect to voltage at the detector output

$$(\text{S/N})_2 = \frac{\langle S_{\text{u}_2}\rangle}{\sqrt{\overline{(S_{\text{n}_2} - \overline{S_{\text{n}_2}})^2}}} \tag{40}$$

is related to (S/N) via the relation [11]

$$(\text{S/N})_2 = \frac{(\text{S/N})}{\sqrt{1+2(\text{S/N})}} = \begin{cases} (\text{S/N}), & (\text{S/N}) \ll 1, \\ \sqrt{(\text{S/N})/2}, & (\text{S/N}) \gg 1. \end{cases} \tag{41}$$

The signal-to-noise ratio at the linear detector output is estimated using the formula

$$(\text{S/N})_1 = \frac{\langle S_{\text{u}_1}\rangle}{\sqrt{\overline{(S_{\text{n}_1} - \overline{S_{\text{n}_1}})^2}}} = \begin{cases} (\text{S/N}), & (\text{S/N}) \ll 1, \\ \sqrt{2(\text{S/N})}, & (\text{S/N}) \gg 1. \end{cases} \tag{42}$$

Let us consider similar relations for a lidar with ideal energy receiver (without reference beam). The transceiving apertures of the lidar and the OCT system are assumed to be equal, and the power of

the sounding pulse is given in the form (28) such that the statistically average current of the useful lidar signal

$$\langle i_u(t)\rangle = \eta \langle P_S\rangle = \eta P_0(0) \langle p_S(\vec{r}_{0\perp}, t)\rangle \tag{43}$$

would reproduce the dependence $S_{u_2}(\vec{r}_{0\perp}, z_0) \sim i_u^2$ for $t = t_0$. Then, taking into account that the dispersion of the shot current in the lidar signal band $\Delta f_p = 1/\tau_p$ is equal to

$$\overline{i_{sh}^2} = 2e\langle i_u\rangle/\tau_p\,, \tag{44}$$

the signal-to-noise ratio in the lidar image of the medium is written as

$$(S/N)_p = \frac{\langle i_u\rangle}{\sqrt{\overline{i_{sh}^2}}} = \sqrt{\frac{\eta W_0 \langle p_S\rangle}{2e}}\,, \tag{45}$$

where $W_0 = P_0(0)\tau_p$ is the sounding-pulse energy. Comparing Eqs. (38) to (42) and Eq. (45), we draw the following conclusions:

1. The dependence of the parameters (S/N) and $(S/N)_p$ on the attenuation coefficient of the useful signal is substantially different: the former varies in proportion with $\langle p_S\rangle$, while the latter varies in proportion with $\sqrt{\langle p_S\rangle}$. This is explained by the fact that in the case of coherent sounding, noises are generated by the reference light beam, whereas in the case of pulsed sounding they are generated by the reflected signal. In the former case they are additive, and in the latter case they are multiplicative.

2. Since in the process of detection of the signal $(i_u + \Delta i_n)$ additive noise is transformed into mutiplicative interference, for $(S/N) > 2$ (see Eq. (41)) the parameter $(S/N)_{1,2}$ varies in proportion with $\sqrt{\langle p_S\rangle}$ similar to $(S/N)_p$.

3. In the case in which excess noises in the OCT system are small compared with shot noises ($\delta \ll 1$) and $(S/N) > 2$, the parameters $(S/N)_{1,2}$ and $(S/N)_p$ depend on the power of the radiation source in a similar manner. However, the contribution from the excess noises increases with i_r and becomes governing for $i_r \gg e/\tau_c$. In this case, the signal-to-noise ratio in the OCT system no longer depends on the illumination-beam power. *

4. In the case $\delta \ll 1$, $(S/N) > 2$, the signal-to-noise ratio in the systems of coherent sounding (with a quadratic detector of the video signal) and pulsed sounding (with an ideal energy receiver and without a reference beam) is the same ($(S/N)_2 = (S/N)_p$) if $2\beta W_0 = P_0\tau_c$. With allowance for Eq. (21), the condition of equivalence of coherent and pulsed sounding is written as

$$W_0 = P_0 c\tau_c t_c/(4z_c) \tag{46}$$

or

$$\overline{P_0} = P_0/(2N_e), \quad N_e = z_c/\Delta z_e\,, \tag{47}$$

where $\overline{P_0} = W_0/t_c$ is the average power of the pulsed radiation source, z_c and t_c are the length and formation time of an image line, respectively, N_e is the number of expansion elements in a line, and $\Delta z_e = c\tau_c/2$ is the element size. If we assume that P_0 is the half-power of a continuous light source, then, according to Eq. (47), in the case of coherent sounding the energy spent on the formation of an image line is a factor of $4N_e$ greater than that spent on the formation of an image line in the case of pulsed sounding.

5. A MODEL OF RANDOM REALIZATIONS OF A REFLECTED SIGNAL

It is assumed that large-scale inhomogeneities of the medium scatter light only forward, while the reflected signal results from the light scattering by small-scale fluctuations of permittivity (the volume-

*In principle, excess noises can be compensated by creating a special channel for checking the reference-beam power. In operating devices they are suppressed in a simpler manner, i. e., attenuating the reference beam.

scattering signal) and local inhomogeneities (objects) with a given scattering cross section.

In the scalar formulation, the problem of the light-wave field $u(\vec{r}, t)$ in a medium with inhomogeneous distribution ε of the type (1) is reduced to solving the equation

$$\left[\Delta + k^2(1 + \varepsilon_1 + \varepsilon_2)\right] V = 0 \tag{48}$$

for the complex amplitude of the harmonic component of the field

$$V(\vec{r}, \omega) = \frac{1}{2\pi} \int_{-\infty}^{\infty} u(\vec{r}, t)\, \mathrm{e}^{-i\omega t} dt \tag{49}$$

for $k = \omega\sqrt{\langle\varepsilon\rangle}\,/\,c_0$ and the appropriate boundary conditions (c_0 is the velocity of light in vacuum).

Let us use f_0 and f_S to denote the spectra of random realizations of the sounding and scattered signals

$$f_{0,S}(\omega) = \frac{1}{2\pi} \int_{-\infty}^{\infty} v_{0,S}(t)\, \mathrm{e}^{-i\omega t} dt \tag{50}$$

and present V in the form

$$V = f_0(\omega)\, V_0(\vec{r}, \omega) + V_S(\vec{r}, \omega)\,, \tag{51}$$

where V_0 is the solution of Eq. (48) for $\varepsilon_2 \equiv 0$ and the boundary condition on the lidar aperture

$$V_0 = M(\vec{r}_\perp), \tag{52}$$

and V_S is the field scattered by the small-scale inhomogeneities. In the linear approximation with respect to ε_2, V_S satisfies the equation

$$\left[\Delta + k^2(1 + \varepsilon_1)\right] V_S = -4\pi\rho_S\,, \tag{53}$$

which differs from the equation for V_0 only by the presence of sources with the density

$$\rho_S = \frac{k^2}{4\pi} f_0(\omega)\, \varepsilon_2(\vec{r})\, V_0(\vec{r}, \omega) \tag{54}$$

on its right-hand side.

The amplitude of the mode excited by this source in an optical waveguide is found using the reciprocity theorem:

$$f_S(\omega) = \frac{2\pi}{ik} \int_V \rho_S\, V_0\, d^3\vec{r} = K(\omega)\, f_0(\omega), \tag{55}$$

$$K(\omega) = -\frac{ik}{2} \int_V \varepsilon_2(\vec{r})\, V_0^2(\vec{r}, \omega)\, d^3\vec{r}. \tag{56}$$

(The reflection of the sounding signal from the fiber end is not allowed for in the above formula.)

From Eqs. (15a), (55), and (50), allowing for the relation

$$\left\langle f_0(\omega)\, f_0^*(\omega')\right\rangle = S_0(\omega)\, \delta(\omega' - \omega) \tag{57}$$

we find

$$i_u(t_0) = \eta\sqrt{2/n} \int_{-\infty}^{\infty} S_0(\omega)\, K(\omega) \mathrm{e}^{-i\omega t_0} d\omega\,. \tag{58}$$

The expression for the signal arriving from the point $\vec{r}_i$ from a single inhomogeneity is obtained from Eqs. (58) and (56) by the formal substitution

$$\varepsilon_2 = \frac{4\pi}{k^2} A_s \cdot \delta(\vec{r} - \vec{r}_i), \tag{59}$$

where A_s is the scattering amplitude related to the differential scattering cross section and effective scattering area (ESA) by [12]

$$A_s A_s^* = \Sigma_{\text{diff}} = \text{ESA}/4\pi\,. \tag{60}$$

The above formulas indicate that to find the useful signal i_u, we must have a model of the field of the monochromatic wave beam V_0 in a medium with large-scale inhomogeneities. Let us write this field in the form

$$V_0 = A(\vec{r}) \exp\left(-ik'z - ik'\zeta(\vec{r})\right), \tag{61}$$

where A and $k'\zeta$ are the random values of the wave amplitude and phase at the point $\vec{r}$, $k' = \omega/c$, $c = c_0/\text{Re}\sqrt{\langle\varepsilon\rangle}$ is the average velocity of light in the medium, and it is assumed for simplicity that A and ζ are frequency independent in the sounding-signal band. In this case, we ignore the signal shape distortions related to dispersion and the frequency dependence of the wave size of the aperture.

Then from Eqs. (58), (56), (61), and (7), with allowance for the quasimonochromatic nature of the illumination source, we obtain the expressions

$$i_u = \text{Re} I_u\,, \tag{62}$$

$$I_u = -i\frac{\omega_0}{c_0}\sqrt{\langle\varepsilon\rangle}\sqrt{\frac{n}{2}}\,i_r \int\limits_V \varepsilon_2(\vec{r})\, A^2(\vec{r})\, b_0(\tau)\, e^{i\omega_0\tau} d^3\vec{r}, \tag{63}$$

$$\tau = t_0 - \tfrac{2}{c}\left[z + \zeta(\vec{r})\right], \tag{64}$$

which establish a direct relation between i_u and the autocorrelation function of the sounding signal. The image is formed as a result of visualization of the signals S_{u_1} or S_{u_2}, which are obtained after the detection of current i_u. These signals are expressed in terms of I_u in the form

$$S_{u_1} = \frac{2}{\pi\sqrt{n}\,i_r}\sqrt{I_u \cdot I_u^*}\,, \qquad S_{u_2} = \frac{1}{2ni_r^2} I_u \cdot I_u^*\,. \tag{65a, b}$$

6. FORMULAS FOR CALCULATING AN IMAGE OF A LOCAL INHOMOGENEITY

The video signals forming an image of a local inhomogeneity ("of a point object") with the given effective scattering area are found from Eqs. (59), (63), (65), and (60):

$$\begin{aligned} S_{u_1} &= 4(2\pi)^{-1/2} k_0^{-1} (\text{ESA})^{1/2} A^2(\vec{r}_i)\, |b_0(\tau_i)|\,, \\ S_{u_2} &= \pi k_0^{-2} (\text{ESA})\, A^4(\vec{r}_i)\, b_0^2(\tau_i), \\ \tau_i &= t_0 - \frac{2}{c}\left[z_i + \zeta(\vec{r}_i)\right], \end{aligned} \tag{66a - c}$$

$k_0 = \omega_0/c$, $c = c_0/\text{Re}\sqrt{\langle\varepsilon\rangle}$, $\vec{r}_i(\vec{r}_{i\perp}, z_i)$ is the point of inhomogeneity location (the formulas are written with allowance for the condition $|\text{Im}\langle\varepsilon\rangle| \ll \text{Re}\langle\varepsilon\rangle$).

From Eq. (66), it is obvious that the useful signal as a function of delay time of the reference signal (t_0) repeats the envelope of the autocorrelation function of the sounding signal (or the envelope squared) and reaches a maximum at $t_0 = t_{0i} = 2(z_i + \zeta)/c$. The amplitude of the useful signal is propor-

tional to the intensity (or the intensity squared) of the illumination field at the point of inhomogeneity location and is the random function $\vec{r}_i$. The quantity t_{0i} also contains the random component $(2\zeta/c)$. Therefore, the error in determining the distance (z_i) from the measured value of t_{0i} depends not only on the coherence time (τ_c) of the emitted signal but also on the phase fluctuations V_0 of the wave at the point $\vec{r}_i$.

To calculate the statistically average video signals, we use the following assumptions:

A. The fluctuations of A and ζ are statistically independent.

B. The scattered component of the field of the illumination beam

$$V_S = V_0 - \langle V_0 \rangle = A_S e^{-i\varphi_S} \tag{67}$$

fluctuates in accordance with the normal law such that its amplitude and phase have the following distributions:

$$p(A_S) = \left(2A_S \Big/ \left\langle A_S^2 \right\rangle\right) \exp\left(-A_S^2 \Big/ \left\langle A_S^2 \right\rangle\right), \qquad p(\varphi_S) = 1/2\pi \quad (0 \le \varphi_S \le 2\pi). \tag{68a, b}$$

C. The probability density ζ can be approximated by the function

$$p(\zeta) = \left(\sqrt{2\pi}\sigma_\zeta\right)^{-1} \exp\left[-(\zeta - \langle\zeta\rangle)^2 \Big/ 2\sigma_\zeta^2\right]. \tag{69}$$

D. The envelope of the autocorrelation function of the sounding signal has Gaussian shape (see Eq. (16)).

E. The field of large-scale fluctuations of permittivity of the medium (ε_1) is statistically homogeneous in the plane $z = \text{const}$.

Calculating the statistical means of $S_{u_{1,2}}$, we assume that the variable $\vec{r}_{0\perp}$ is one of the arguments of A and ζ (previously, the dependence of these functions on $\vec{r}_{0\perp}$ was not shown explicitly). We also take into account that under the condition (E) the statistical moments $A(\vec{r}_{0\perp}, \vec{r}_\perp, z)$ and $\zeta(\vec{r}_{0\perp}, \vec{r}_\perp, z)$ depend only on the variables $\vec{\rho} = \vec{r}_{0\perp} - \vec{r}_\perp$ and z. For the mean-square amplitude of the field V_0 and the intensity of its nonscattered component, we use the special notations

$$E(\vec{\rho}, z) = \frac{1}{2}\left\langle A^2(\vec{r}_{0\perp}, \vec{r}_\perp, z)\right\rangle, \tag{70}$$

$$E_{ns}(\vec{\rho}, z) = \frac{1}{2}\left|\langle V_0(\vec{r}_{0\perp}, \vec{r}_\perp, z)\rangle\right|^2 \tag{71}$$

and note that under the condition (B) the following relation is fulfilled:

$$\left\langle A^4\right\rangle \Big/ 4 = 2E^2 - E_{ns}^2. \tag{72}$$

With allowance for conditions A, C, D, and Eq. (72), the statistically average images $J_{1,2} = \langle S_{u_{1,2}}\rangle$ are presented as

$$J_1(\vec{r}_{0\perp}, z) = \frac{8}{\sqrt{2\pi}k_0}(\mathrm{ESA})^{1/2} E(\vec{\rho}_i, z_i)\, b_1(z_0 - z_i,\, z_i), \tag{73}$$

$$J_2(\vec{r}_{0\perp}, z_0) = \frac{4\pi(\mathrm{ESA})}{k_0^2}\left[2E^2(\vec{\rho}_i, z_i) - E_{ns}^2(\vec{\rho}_i, z_i)\right] b_2(z_0 - z_i, z_i), \tag{74}$$

$$b_{1,2}(\Delta z, z_i) = \left[1 + 2\pi\left(\frac{\sigma_\zeta}{\Delta z_{1,2}}\right)^2\right]^{-1/2} \exp\left[-\frac{\pi(\Delta z - \langle\zeta\rangle)^2}{(\Delta z_{1,2})^2 + 2\pi\sigma_\zeta^2}\right], \tag{75}$$

$$z_0 = ct_0/2, \quad \vec{\rho} = \vec{r}_{0\perp} - \vec{r}_{i\perp}, \quad \Delta z_1 = \frac{c\tau_c}{\sqrt{2}}, \quad \Delta z_2 = \frac{c\tau_c}{2}. \qquad (76a-d)$$

The quantity z_i is given as an argument of the functions $b_{1,2}$ because the parameters $\langle\zeta\rangle$ and σ_ζ^2 depend on z_i; $E(\vec{\rho}, z)$ is the distribution of irradiance (statistically average density of the energy flux) in the medium from a continuous radiation source with unit power and directivity characteristics, which are similar to those of the actual illumination source, or, in other words, the irradiance in the illumination beam divided by the source power; E_{ns} is the irradiance by nonscattered light (E and E_{ns} have the dimension $[1/m^2]$).

To calculate the three-dimensional image of inhomogeneity, in addition to the distributions E and E_{ns}, we must know the parameters $\langle\zeta\rangle$ and σ_ζ^2, which are expressed in terms of the time characteristics of the δ-pulse light beam.

Indeed, using Eq. (61), we see that if a source with power $P = W_0\,\delta(t)$ forms the irradiance field $E_\delta(\vec{r}, t)$ in the medium, the probability density ζ is expressed in terms of E_δ as

$$p(\zeta) = E_\delta\left(\vec{r}, \frac{z}{c} + \frac{\zeta}{c}\right)\left(c\int\limits_{-\infty}^{\infty} E_\delta\,dt\right)^{-1}, \qquad (77)$$

and the parameters $\langle\zeta\rangle$ and σ_ζ^2 are related to the time characteristics of the light pulse that arrives at the point $\vec{r}$ via the relations

$$\langle\zeta\rangle = c\bar{t} - z, \quad \bar{t} = \int\limits_{-\infty}^{\infty} t\,E_\delta\,dt \Big/ \int\limits_{-\infty}^{\infty} E_\delta\,dt, \qquad (78a,b)$$

$$\sigma_\zeta^2 = c^2\overline{(\Delta t)^2}, \quad \overline{(\Delta t)^2} = \int\limits_{-\infty}^{\infty} (t-\bar{t})^2 E_\delta\,dt \Big/ \int\limits_{-\infty}^{\infty} E_\delta\,dt. \qquad (79a,b)$$

Note that irradiance in the continuous illumination beam is also expressed in terms of the pulsed irradiance

$$E = \frac{1}{W_0}\int\limits_{-\infty}^{\infty} E_\delta\,dt. \qquad (80)$$

As is obvious from Eq. (73), in the case of linear detection of a signal, the two-dimensional image of the point inhomogeneity repeats the distribution of irradiance (E) in the section of the illumination beam by the plane $z = z_i$. In quadratic detection (see Eq. (74)), it reproduces approximately the squared distribution of irradiance. The absence of one-to-one correspondence between the functions J_2 and E^2 is attributed to the fact that in the case of use of a quadratic detector the spatial fluctuations of the illumination-beam intensity contribute to the statistically average image (enhanced backscattering in a medium with large-scale inhomogeneities [13]). This contribution is a function of the field-fluctuation statistics and is minimal under the condition B, which can be violated if a medium has inhomogeneities similar to short-focus lenses.

In the case of quadratic detection the image is sharper (less blurred). However, its fluctuations are stronger, which is confirmed by the estimates of the signal-variation coefficients:

$$\delta S_{u1,2} = \sqrt{\langle (S_{u1,2} - \langle S_{u1,2}\rangle)^2\rangle} \Big/ \langle S_{u1,2}\rangle\,. \qquad (81)$$

These coefficients are related to the statistical moments of the illumination-field amplitude via the relations

$$\delta S_{u1} = \frac{\sqrt{\langle A^4\rangle - \langle A^2\rangle^2}}{\langle A^2\rangle}, \qquad \delta S_{u2} = \frac{\sqrt{\langle A^8\rangle - \langle A^4\rangle^2}}{\langle A^4\rangle}, \qquad (82a,b)$$

from which, in particular, for $E_{ns} \ll E$ we have

$$\delta S_{u_1} = 1, \qquad \delta S_{u_2} = \sqrt{5}. \tag{83a, b}$$

7. AN IMAGE OF THE MEDIUM WITH CONTINUOUSLY DISTRIBUTED SCATTERERS. THE EQUATION OF IMAGE TRANSFER

As a result of backscattering of an illumination beam from small-scale inhomogeneities of the medium, each inhomogeneity generates the correlation response $i_u \sim b_0(\tau_i)\cos\omega_0\tau_i$ with random amplitude and phase. If the number of inhomogeneities in the resolution element is large, the sum of these responses forms a noise- like signal i_u with statistically mean $\langle i_u\rangle = 0$. After the detection of i_u a regular component appears in the signal. It is calculated by substituting Eq. (63) into Eq. (65) and averaging $S_{u_{1,2}}$ over the field-realization ensembles $\varepsilon_{1,2}$. The statistically average images of the medium are described by the expressions

$$J_2(\vec{r}_{\perp 0}, z_0) = \langle S_{u_2}\rangle = 2\pi^3 k_0^2 \int\limits_V \Phi_2(\vec{r}, 2k_0)\left\langle A^4(\vec{r}_{\perp 0}, \vec{r})\, b_0^2(\tau)\right\rangle d^3\vec{r}, \tag{84}$$

$$J_1 = \langle S_{u_1}\rangle = \sqrt{\frac{2}{\pi}} J_2, \tag{85}$$

where $z_0 = ct_0/2$, Φ_2, and τ are determined from Eqs. (3) and (64). Deriving Eqs. (84) and (85), we assumed the large-scale (ε_1) and small-scale (ε_2) fluctuations of ε to be statistically independent and used the condition of smallness of the correlation radius (l_2) of the small-scale fluctuations compared with the scale of the spatial inhomogeneity $A^2(\vec{r})$ and the size of the resolution element with respect to distance ($c\tau_c/2$). In Eq. (85), we assume that the quadrature components of the current i_u ($\mathrm{Re}I_u, \mathrm{Im}I_u$) are distributed according to the normal law.

In accordance with Eqs. (84) and (85), the images $J_{1,2}$ bear information on the spectral density of fluctuations ε with spatial frequency $2k_0$.

The function of volume scattering (β) of a randomly inhomogeneous medium (differential cross section of the scattering of its volume unit) is expressed in terms of the total spectrum of the permittivity fluctuations

$$\Phi(\vec{r}, \kappa) = \Phi_1(\vec{r}, \kappa) + \Phi_2(\vec{r}, \kappa) \tag{86}$$

in the form [14]

$$\beta(\vec{r}, \gamma) = \frac{\pi}{2} k_0^4 \Phi\left(\vec{r}, 2k_0 \sin\frac{\gamma}{2}\right) \tag{87}$$

(γ is the scattering angle). Therefore, with allowance for the condition $\Phi_1(\vec{r}, 2k_0) \equiv 0$, in Eq. (84) we assume

$$\Phi_2(\vec{r}, 2k_0) = \frac{2}{\pi k_0^4}\beta(\vec{r}, \pi) = \frac{1}{2\pi^2 k_0^4}\sigma_0(\vec{r}), \tag{88}$$

where

$$\sigma_0(\vec{r}) = 4\pi\beta(\vec{r}, \pi) \tag{89}$$

is the backscattering coefficient (the effective area of backscattering of a unit volume of the medium). If we use the expression for $\langle A^4 b_0^2\rangle$ from Section 5, J_2 can be written as

$$J_2(\vec{r}_0) = \int\limits_V \sigma_0(\vec{r})\, Q(\vec{r}_0 - \vec{r})\, d^3\vec{r}, \tag{90}$$

$$Q(\vec{\rho}) = 4\pi k_0^{-2}\left[2E^2(\vec{\rho}_\perp, z_0) - E_{ns}^2(\vec{\rho}_\perp, z_0)\right] b_2(\rho_z, z_0), \tag{91}$$

where $\vec{r} = \vec{r}_\perp + z \cdot \vec{z}_0$, $\vec{r}_0 = \vec{r}_{0\perp} + z_0 \cdot \vec{z}_0$, $\vec{\rho} = \vec{\rho}_\perp + \rho_z \cdot \vec{z}_0$, $z_0 = \dfrac{ct_0}{2}$.

Equation (90) is a three-dimensional analog of the image-transfer equation [6, 9], and the function $Q(\vec{\rho})$ is the three-dimensional function of point blurring (FPB). The statistically average image of the point inhomogeneity (determined by Eq. (74)) is obtained from Eq. (90) using the formal replacement

$$\sigma_0(\vec{r}) = (\text{ESA})\,\delta(\vec{r} - \vec{r}_i) \tag{92}$$

and is expressed via Q as

$$J_2(\vec{r}_0) = (\text{ESA}) \cdot Q(\vec{r}_0 - \vec{r}_i). \tag{93}$$

Therefore, the statistically average images of local inhomogeneity and distributed scatterers are described by the universal formulas (90) and (91). However, their random realizations differ markedly by the fluctuation level. The signals S_{u_1} and S_{u_2} arriving from the small-scale inhomogeneities are distributed as the amplitude and intensity of normal noise, respectively. They are characterized by the variation coefficients

$$\delta S_{u_1} \cong 0.523\,, \quad \delta S_{u_2} = 1\,, \tag{94}$$

which are approximately two times smaller than the coefficients (83).

8. THE FUNCTION OF POINT BLURRING

As is obvious from Eqs. (90) and (91), to study the regular component of the image (J_2), we must have the FPB model, which can be developed on the basis of the data on irradiance distribution in a continuous illumination beam (E) and the parameters $\bar{t}$ and $\overline{(\Delta t)^2}$ characterizing the group delay and blurring of the δ-pulse signal as it passes through the scattering medium.

Calculating the FPB, we must allow for the presence of the focusing system between the emitting end of an optical waveguide and the boundary of the medium. For this purpose it suffices to replace M in Eq. (52) by the function $M_0(\vec{r}_\perp)$, which describes the distribution of the field V_0 at the output of the focusing system and satisfies the normalization condition

$$\iint\limits_{-\infty}^{\infty} |M_0|^2\, d^2\vec{r}_\perp = 1. \tag{95}$$

Recall that V_0 is the wave beam field in a fictitious medium without small-scale inhomogeneities. This medium is characterized by the function of volume scattering $\beta_1(z,\gamma) \sim \Phi_1$ (see Eqs. (86) and (87)), the small-angle scattering index

$$\sigma_1(z) = 2\pi \int\limits_0^\pi \beta_1(z,\gamma) \sin\gamma\, d\gamma = \frac{k_0^2}{2} \int\limits_0^\infty B_{\varepsilon_1}(z,\rho)\, d\rho\,, \tag{96}$$

the small-angle scattering indicatrix

$$x_1(z,\gamma) = \beta_1/\sigma_1\,, \tag{97}$$

the attenuation index $\alpha(z)$, and the effective absorption index

$$\kappa_1(z) = \alpha(z) - \sigma_1(z). \tag{98}$$

It is assumed that α coincides with the attenuation index of the actual medium (which allows us to take into account the energy losses of the illumination beam due to the light scattering from small- scale inhomogeneities).

To divide the measured function of volume scattering of the medium into the high-directivity (β_1)

and weakly anisotropic parts, it is expedient to use the relation

$$\beta_1 = \begin{cases} \beta, & \gamma < \pi/4, \\ 0, & \gamma > \pi/4, \end{cases} \tag{99}$$

or to describe β_1 using a function that approximates β in the region $0 < \gamma < \pi/4$ and rapidly falls off exponentially for $\gamma > \pi/4$. In this case, the effective absorption index of the medium (κ_1) and the small-angle scattering index (σ_1) are related to the index of true absorption $\kappa(z)$ and the total scattering index $\sigma(z)$ via the relations [9]

$$\kappa_1 = \kappa + \varphi_{45}\sigma\,, \qquad \sigma_1 = (1 - \varphi_{45})\sigma\,,$$
$$\varphi_{45} = \int\limits_{\pi/4}^{\pi} \beta \sin\gamma\, d\gamma \Big/ \int\limits_{0}^{\pi} \beta \sin\gamma\, d\gamma \tag{100a - c}$$

(φ_{45} is the fraction of light scattered by an elementary volume of the medium to the angles $\gamma > 45°$). For the Heny–Greenstein scattering indicatrix, which is usually used in the problems of optics of tissues, the relation

$$\varphi_{45} = 1 - \langle \cos\gamma \rangle \tag{101}$$

is fulfilled with very high accuracy ($\langle \cos\gamma \rangle$ is the average cosine of the indicatrix). Therefore, in the future we shall identify the parameter κ_1 with the transport attenuation index

$$\kappa_1 = \alpha_t = \sigma_t + \kappa, \qquad \sigma_t = (1 - \langle \cos\gamma \rangle)\sigma\,. \tag{102}$$

On the basis of solution of the radiative transfer equation (RTE) in the small-angle approximation, the distribution of E in a stratified turbid medium is presented as [15]

$$E(\vec{\rho}_\perp, z) = \iint\limits_{-\infty}^{\infty} C(\vec{h}, z) e^{i\vec{h}\vec{\rho}_\perp} d^2\vec{h}, \tag{103}$$

$$C(\vec{h}, z) = C_{ns}(\vec{h}, z) \exp\left[\int\limits_0^z \sigma_1(z - z')\overline{x_1}(z - z', hz')dz' \right], \tag{104}$$

$$C_{ns}(\vec{h}, z) = \frac{e^{-\tau_\alpha}}{(2\pi)^2} \iint\limits_{-\infty}^{\infty} M_0\left(\vec{r}_\perp + \frac{\vec{h}z}{2k_0}\right) M_0^*\left(\vec{r}_\perp - \frac{\vec{h}z}{2k_0}\right) e^{-i\vec{h}\vec{r}_\perp} d^2\vec{r}_\perp, \qquad \tau_\alpha = \int\limits_0^z \alpha(z)\, dz, \tag{105a, b}$$

$$\overline{x_1}(z, p) = \int\limits_0^\infty x_1(z, \gamma)\, J_0(p\gamma)\gamma\, d\gamma \Big/ \int\limits_0^\infty x_1(z, \gamma)\gamma\, d\gamma = \frac{k_0^2}{2\sigma_1} \int\limits_0^\infty B_{\varepsilon_1}\left(z, \sqrt{\rho^2 + (p/k_0)^2}\right) d\rho. \tag{106}$$

The distribution of irradiance E_{ns} created by the nonscattered component of the light beam is found by replacing Eq. (104) by Eq. (105) on the right-hand side of Eq. (103).

In particular, for the focused Gaussian beam, assuming that

$$M_0 \sim \exp\left(-\frac{r_\perp^2}{2a_0^2} + \frac{ik_0 r_\perp^2}{2z_f} \right) \tag{107}$$

and the focusing system aperture is shifted from the boundary of the medium by the distance Δz, we obtain

$$E_{ns}(\vec{\rho}_\perp, z) = \frac{1}{\pi a^2} \exp\left(-\tau_\alpha - \frac{\rho_\perp^2}{a^2} \right), \tag{108}$$

$$a^2 = a_0^2\left(1 - \frac{z+\Delta z}{z_f}\right)^2 + \left(\frac{z+\Delta z}{k_0 a_0}\right)^2. \tag{109}$$

We use a_0 to denote the effective radius of the beam at the focusing system aperture, z_f is the distance from the aperture to the focusing point, and a is the effective radius of the beam at the depth z.

Using the appropriate approximation for $x_1(\gamma)$, we present the total irradiance (E) in the form of a single integral, which makes it possible to develop sufficiently simple numerical algorithms for calculating the FPB and J_2. For approximate estimates (to which we confine ourselves in this paper) one can use the simplest (although rough) expression for E in the form of the sum of E_{ns} and the Gaussian distribution of irradiance whose parameters are chosen such that the integral characteristics of the beam (total power and distribution variance of irradiance in its cross section) are described by the formulas [6, 16] of the small-angle diffusion approximation of the theory of radiation transfer:*

$$E = E_{ns} + E_S, \qquad E_S = \frac{P_S}{\pi a_S^2}\exp\left(-\frac{\rho_1^2}{a_S^2}\right), \qquad P_S = e^{-\tau_t} - e^{-\tau_\alpha},$$

$$a_S^2 = a^2 + \frac{1}{3}\left\langle\gamma^2\right\rangle \tau_\sigma z^2 \Big/ \left(1 - e^{-\tau_\sigma}\right), \tag{110a-g}$$

$$\left\langle\gamma^2\right\rangle = \int_0^{\pi/4} \gamma^2 x_1(\gamma)\sin\gamma\, d\gamma \Big/ \int_0^{\pi/4} x_1(\gamma)\sin\gamma\, d\gamma,$$

$$\tau_t = \int_0^z \alpha_t(z')\, dz', \qquad \text{and} \qquad \tau_\sigma = \sigma_1 z.$$

Here E_S is the irradiance of the plane $z = \text{const}$ by scattered light, P_S is the power of the scattered component of the light beam, a_S^2 is the variance of irradiance distribution in a light spot that is formed by scattered light, and $\langle\gamma^2\rangle$ is the variance of the high- directivity part of the scattering indicatrix.

To estimate the parameters $\langle\zeta\rangle$ and σ_ζ^2 that enter Eqs. (75) and (91), we use the formulas resulting from the self-similarity solution of the RTE in the small-angle diffusion approximation [17, 18]:

$$\langle\zeta\rangle_{\vec{\rho}_\perp=0} = \frac{\langle\gamma^2\rangle}{20}\tau_\sigma z,$$

$$\left[\sigma_\zeta^2\right]_{\vec{\rho}_\perp=0} = \frac{\langle\gamma^2\rangle^2}{560}\tau_\sigma^2 z^2. \tag{111a,b}$$

Although, unlike Eqs. (103)–(106), Eqs. (110) and (111) are written for the case $\sigma_1 = \text{const}$, they are rather simply generalized to the arbitrarily stratified medium.

9. THE FREQUENCY-CONTRAST CHARACTERISTIC (FCC) OF THE OCT SYSTEM

Equation (90) allows us to consider the image $J_2(\vec{r})$ as a spatial signal, which results from the passage of the signal $\sigma_0(\vec{r})$ through a linear filter with pulsed response $Q(\vec{\rho})$ and frequency characteristic

$$M(\vec{h}, z_0)e^{-i\psi} = \iiint_{-\infty}^{\infty} Q(\vec{\rho}, z_0)e^{-i\vec{h}\vec{\rho}}d^3\vec{\rho} \Big/ \iiint_{-\infty}^{\infty} Q d^3\vec{\rho}, \tag{112}$$

*A similar method was used in [17] to improve the self-similarity solutions of the transfer equation.

which is called optical transfer function, and its absolute value M is called the frequency-contrast characteristic. If we ignore the dependence of the parameters $\langle\zeta\rangle$ and σ_ζ^2 on $\vec{\rho}_\perp$ and present $\vec{h}$ in the form $\vec{h} = \vec{h}_\perp + h_z \cdot \vec{z}_0$, then, under the condition of axial symmetry of the illumination beam, from Eqs. (91) and (112) we obtain

$$M(\vec{h}, z_0) = M_\perp(\vec{h}_\perp, z_0)\, M_z(h_z, z_0),$$

$$M_\perp(\vec{h}, z_0) = f(h_\perp, z_0)/f(0, z_0), \quad h_\perp = \left|\vec{h}_\perp\right|,$$

$$f(h_\perp, z_0) = 2\pi \int_0^\infty \left[2E^2(\rho_\perp, z_0) - E_{\text{ns}}^2(\rho_\perp, z_0)\right] J_0(h_\perp \rho_\perp)\rho_\perp\, d\rho_\perp, \tag{113a-e}$$

$$M_z(h_z, z_0)\mathrm{e}^{-i\psi} = \int_{-\infty}^{\infty} b_2(\rho_z, z_0)\mathrm{e}^{-ih_z\rho_z} d\rho_z \Big/ \int_{-\infty}^{\infty} b_2\, d\rho_z .$$

According to Eqs. (90) and (113), when observing a layer of the medium with backscattering coefficient

$$\sigma_0(\vec{r}_\perp, z) = \overline{\sigma_0}\left(1 + m_0 \cos \vec{h}_\perp \vec{r}_\perp\right) \tag{114}$$

the image of this layer

$$J_2(\vec{r}_{0\perp}, z_0) = \overline{J_2}\left[1 + m \cos \vec{h}_\perp \vec{r}_{0\perp}\right] \tag{115}$$

reproduces the variations of σ_0 with contrast

$$m = m_0 M_\perp \tag{116}$$

if the layer thickness is greater than the size of the resolution element with respect to distance. Therefore, $M_\perp$ is considered to be the contrast transfer coefficient of the sinusoidal component of distribution $\sigma_0(\vec{r}_\perp)$.

The average "brightness" of the image $\overline{J_2}$, as the FCC, is expressed in terms of the function f:

$$\overline{J_2} = \overline{\sigma_0} \int_V Q\, d^3\vec{r} = 4\pi\overline{\sigma_0} c\tau_c k_0^{-2} f(0, z_0). \tag{117}$$

Using Eqs. (108)–(110) and Eq. (113d), we write this function in the form

$$\begin{aligned} f(h_\perp, z_0) &= \frac{\mathrm{e}^{-2\tau_t}}{\pi a^2}\left[\frac{1}{2}\mathrm{e}^{-2\tau_\sigma - (h_\perp a)^2/8} + \right. \\ &+ \left. \frac{4\mathrm{e}^{-\tau_\sigma}(1-\mathrm{e}^{-\tau_\sigma})}{1+\varphi}\mathrm{e}^{-\frac{\varphi}{4(1+\varphi)}(h_\perp a)^2} + \frac{(1-\mathrm{e}^{-\tau_\sigma})^2}{\varphi}\mathrm{e}^{-\frac{\varphi}{8}(h_\perp a)^2}\right], \\ \varphi &= a_S^2 \Big/ a^2 = 1 + \frac{1}{C}\cdot\tau_\sigma^3\left(1-\mathrm{e}^{-\tau_\sigma}\right)^{-1}, \\ C &= 3(\sigma_1 a)^2 \Big/ \left\langle\gamma^2\right\rangle, \qquad \tau_\sigma = \sigma_1 z_0, \qquad \tau_t = \int_0^{z_0} \alpha_t\, dz. \end{aligned} \tag{118a-e}$$

The results of calculation of $M_\perp$ using Eqs. (113b) and (118a) are shown in Fig. 2 in the form of the curves presenting the FCC dependence on the optical depth τ_σ at which the observed layer of the medium is located. Each curve corresponds to a certain value of the parameter C and the given value of $l_\perp/2a$, where $l_\perp = 2\pi/h_\perp$ is the scale of the inhomogeneity σ_0 and $2a$ is the diameter of the light spot formed by nonscattered light in the plane $z = z_0$. We ignore the dependence of a on z_0, assuming that $z_0 \ll \Delta z$,

$\Delta z \cong z_f$, and $a \cong (z_f/k_0 a_0)$ (see Eq. (109)).

The curves in Fig. 3 illustrate the dependence of $\lg M_\perp$ on the absolute values of z_0 (in mm) and $l_\perp$ (in μm) with the values of $\langle\gamma^2\rangle$ and σ_1 typical of skin [19].

Using the data in Fig. 2, we conclude that it is possible to observe the internal structure of tissues with sufficiently high transverse resolution ($l_\perp < 20a$) at optical depths $\tau_\sigma < \tau_\sigma^0 \sim 5 \div 10$. We should note the nonmonotonic behavior of the dependence of τ_σ^0 on C (which is proportional to σ_1^2): τ_σ^0 is minimal for $C \sim 1$ and increases as C varies toward larger or smaller values. Such a dependence of τ_σ^0 on C is explained by the competition of two phenomena that influence the resolution: (1) in a more transparent medium, the confocal observation gives a higher resolution gain; (2) the optical depth τ_σ, at which the illumination beam is broadened the given number of times, increases with the scattering index as $\sigma_1^{2/3}$ (see Eq. (110d)). In this case, the absolute values of the depth of inhomogeneity visibility τ_σ^0/σ_1 increase monotonically as σ_1 decreases (see Fig. 3).

The contrast losses in observation of the layered structures in the tissue are characterized by the function M_z. The image of the stratified medium with backscattering coefficient

$$\sigma_0(z) = \overline{\sigma_0}(1 + m_0 \cos h_z z) \tag{119}$$

has the form

$$J_2(z_0) = \overline{J_2}[1 + m\cos(h_z z_0 - \psi)]. \tag{120}$$

It reproduces distribution (119) with contrast $m = m_0 M_z$ and spatial shift $\Delta z_0 = \psi/h_z$, which are determined from Eqs. (75), (90), and (113) as

$$M_z = \exp\left[-(h_z/h_z^0)^2\right],$$

$$h_z^0 = 2\sqrt{\pi}\left[\left(\frac{c\tau_c}{2}\right)^2 + 2\pi\sigma_\zeta^2\right]^{-1/2}, \tag{121a-c}$$

$$\Delta z_0 = \langle\zeta\rangle.$$

According to Eq. (121a), the coefficient of contrast transfer M_z exceeds $1/e$ if the spatial scale of the observed structure $l_z = 2\pi/h_z$ satisfies the condition

$$l_z > l_z^0 = 2\pi/h_z^0. \tag{122}$$

In the initial interval of optical depths when the scatter of photons over the scattering paths is small compared with the coherence length of the sounding signal, $l_z^0 = \sqrt{\pi}(c\tau_c/2)$. As is obvious from Eqs. (111b) and (122), the substantial blurring of the coherence function that leads to an increase in l_z^0 (and a decrease in h_z) by a factor of 2 occurs at the optical depth

$$\tau_\sigma = \sigma_1 z_0 = 2.9\sqrt{\sigma_1 c\tau_c/\langle\gamma^2\rangle}. \tag{123}$$

For example, if $\langle\gamma^2\rangle = 0.03$ and $c\tau_c/2 = 10$ μm, then Eq. (123) yields $\tau_\sigma = 10.6$ ($z_0 = 0.53$ mm) for $\sigma_1 = 20$ mm^{-1}; $\tau_\sigma = 7.5$ ($z_0 = 0.75$ mm) for $\sigma_1 = 10$ mm^{-1}. The dependence of l_z^0 on the depth of location of the observed layer of tissue (for the above parameter values) is shown in Fig. 4.

The light scattering from large-scale inhomogeneities leads to a videosignal delay by time $\langle\zeta\rangle/c$, which results in a systematic error in determination of the distance to the element of the medium from which the signal arrives: the distance is increased by $\Delta z_0 = \langle\zeta\rangle$. The dependence of Δz_0 on z_0 calculated by Eq. (111a) is shown in Fig. 4.

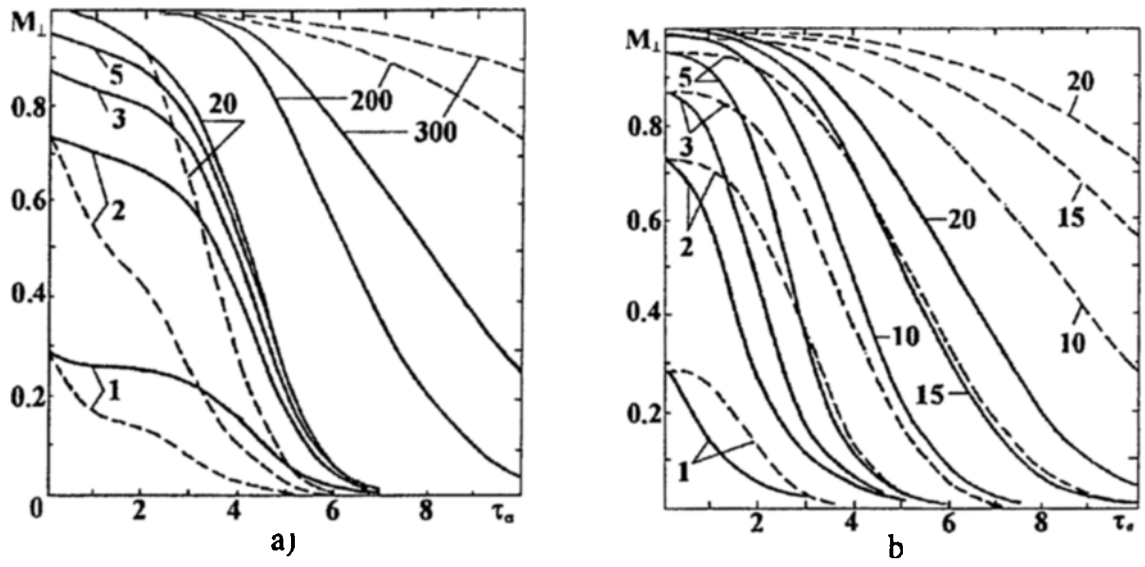

Fig. 2. Frequency-contrast characteristics of $M_\perp$ as a function of $\tau_\sigma = \sigma_1 z_0$ for different parameters $C = 3(\sigma_1 a)^2/\langle\gamma^2\rangle$: a) $C = 0.01$ are the solid curves and $C = 0.1$ is the dashed curve; b) $C = 1.0$ are the solid curves and $C = 10$ is the dashed curve; the figures denote the values of $l_\perp/2a$; $l_\perp = 2\pi/h_\perp$ is the scale of inhomogeneity of the backscattering coefficient, and $2a$ is the focal-spot diameter.

10. ATTENUATION OF THE USEFUL SIGNAL AND LIMITING VISIBILITY DEPTHS

The depth of visibility of the internal structure of tissues can be limited not only by contrast losses but also by attenuation of the average "brightness" of the image ($\overline{J_2}$). Using Eqs. (29), (117), and (118a), we present $\overline{J_2}$ in the form

$$\overline{J_2} = \langle\overline{pS}\rangle \tag{124}$$

in terms of the average coefficient of signal transfer, which is determined from the formulas

$$\langle\overline{pS}\rangle = \overline{\sigma_0} c\tau_c (k_0 a)^{-2} e^{-2\tau_t} p(\tau_\sigma),$$

$$p(\tau_\sigma) = e^{-2\tau_\sigma} + \frac{8}{1+\varphi} e^{-\tau_\sigma}(1 - e^{-\tau_\sigma}) + \frac{2}{\varphi}(1 - e^{-\tau_\sigma})^2. \tag{125a, b}$$

The results of calculation of $p(\tau_\sigma)$ for several values of the parameter C are shown in Fig. 5. As is obvious from the figure, the region of exponential attenuation of the signal is clearly observed only for C below 1 when the ratio between the beam diameter and the photon free path is smaller than the r.m.s. angle of the beam deflection in an elementary scattering event. The signal decreases rapidly with optical depth as the beam radius or the scattering index of the medium decreases. However, its absolute values increase with the power of a signal arriving from the front tissue layer. Under the conditions

$$\tau_\sigma \gg 1 \qquad \text{and} \qquad \tau_\sigma^3 > C > \tau_\sigma^3 e^{-2\tau_\sigma}, \tag{126a, b}$$

to estimate $\langle\overline{pS}\rangle$, we can use the simple asymptotic formula

$$\langle\overline{pS}\rangle = \frac{12}{\langle\gamma^2\rangle}\left(\frac{\overline{\sigma_0}}{\sigma_1}\right)\left(\frac{c\tau_c}{2z_0}\right)(k_0 z_0)^{-2} e^{-2\tau_t}. \tag{127}$$

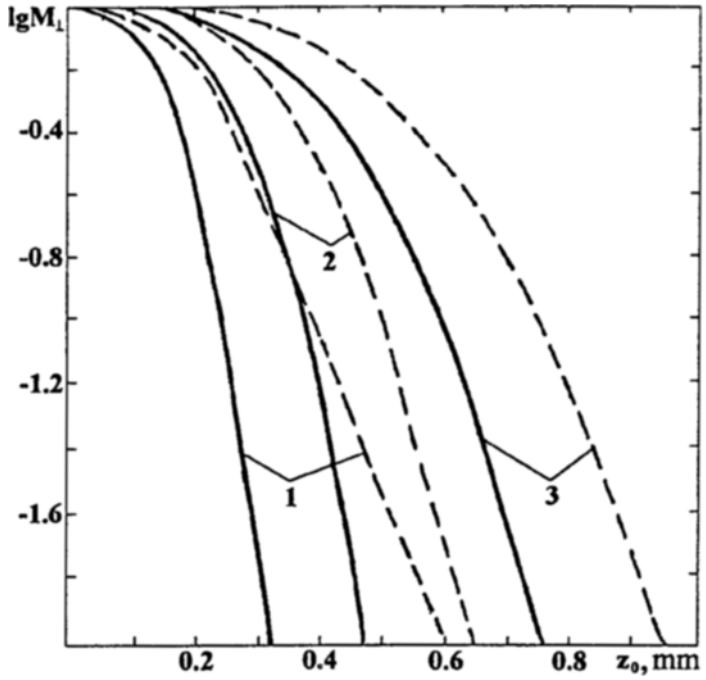

Fig. 3. Frequency-contrast characteristics of $M_\perp$ for the skin- type medium as a function of location depth of the observed tissue layer (mm): $2a = 15$ μm; $\langle\gamma^2\rangle = 0.03$ ($\langle\cos\gamma\rangle = 0.9$); $\sigma_1 = 20$ mm^{-1} are the solid curves, $\sigma_1 = 10$ mm^{-1} is the dashed curve; $l_\perp = 2\pi/h_\perp = 75$ μm are curves 1, 150 μm are curves 2, and 300 μm are curves 3.

Note that for $\langle\cos\gamma\rangle > 0.8$ the optical characteristics of the medium with the Heny–Greenstein scattering indicatrix are related as

$$\sigma_1 = \langle\cos\gamma\rangle\sigma\,, \qquad \overline{\sigma_0} \cong \sigma_t = (1 - \langle\cos\gamma\rangle)\sigma,$$
$$\langle\gamma^2\rangle \cong 0.3(1 - \langle\cos\gamma\rangle), \tag{128a – c}$$

which allow us to exclude the parameters $\overline{\sigma_0}$, σ_1, and $\langle\gamma^2\rangle$ from Eq. (127) and write it in the form

$$\langle\overline{ps}\rangle = \left(\frac{c\tau_c}{2z_0}\right)\left(\frac{\lambda_0}{z_0}\right)^2 e^{-2\tau_t} \Big/ \langle\cos\gamma\rangle\,, \tag{129}$$

where $\lambda_0 = c/f_0$, c is the velocity of light in the medium, and $\tau_t = (\sigma_t + k)z_0$ is the transport depth from which the scattered signal arrives.

As is obvious from Eqs. (125a) and (129), the transfer coefficient of the signal that is reflected from the uppermost layer of the tissue is equal to

$$\langle\overline{ps}(z{=}0)\rangle = \sigma_t c\tau_c (k_0 a)^{-2}, \tag{130}$$

and the power losses in the case of direct and back passage of the signal through a tissue layer with

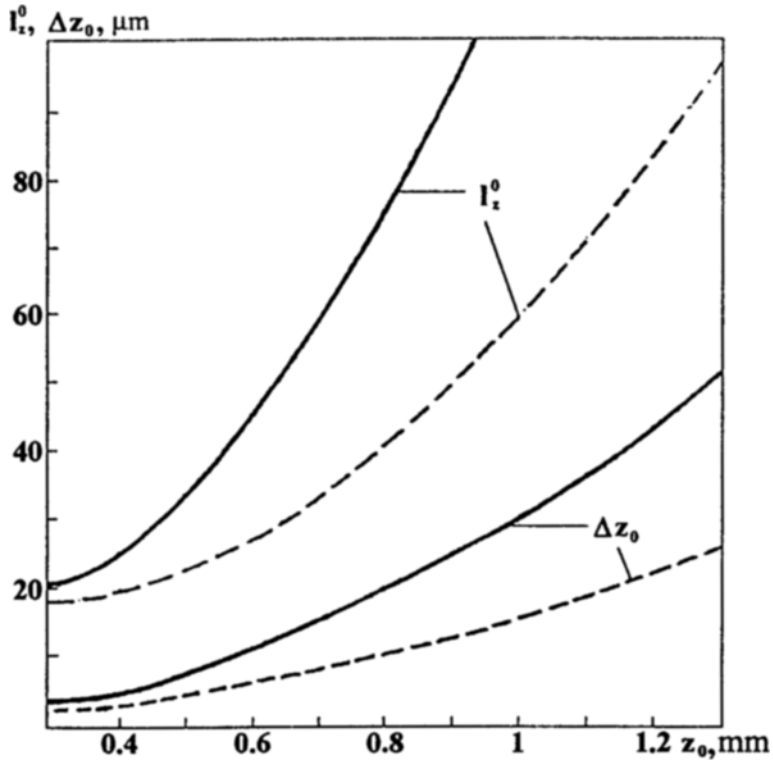

Fig. 4. Systematic error in determination of the distance (Δz_0) and minimum period of the contrastly mapped layered structure (l_z^0) as a function of the sounding depth z_0: $\langle\gamma^2\rangle = 0.03$; $(c\tau_c/2) = 10$ μm, $\sigma_1 = 20$ mm^{-1} are plotted by solid curves and $\sigma_1 = 10$ mm^{-1} are plotted by dashed curves.

thickness z_0 are determined as

$$\langle\overline{ps}\rangle / \langle\overline{ps}(z{=}0)\rangle = 20\left(\frac{a}{z_0}\right)^2 \frac{e^{-2\tau_t}}{\langle\cos\gamma\rangle\tau_t}. \tag{131}$$

For $\sigma_t = 1$ mm^{-1}, $k \ll \sigma_t$, $c\tau_c/2 = 10$ μm, $\lambda_0 = 0.8$ μm, $2a = 15$ μm, $\langle\cos\gamma\rangle = 0.9$, and $z_0 = 1$ mm, Eqs. (130) and (131) give

$$\langle\overline{ps}(z{=}0)\rangle = 5.8 \cdot 10^{-6}, \qquad \langle\overline{ps}\rangle / \langle\overline{ps}(z{=}0)\rangle = 1.7 \cdot 10^{-4}.$$

This example shows that losses due to propagation of light in a tissue are a small fraction of the general losses, and the exponential attenuation of light exerts a relatively weak influence on the average brightness of the image of deep layers of a tissue.

After the replacement $\overline{\sigma_0} \to \sigma_0(\vec{r}_0)$, $\overline{J_2} \to J_2(\vec{r}_0)$, Eqs. (124) and (127) can also be used to calculate the images of large-scale inhomogeneities of the backscattering coefficient if their transverse dimension is

$$l_\perp > z_0\sqrt{0.1 \cdot \tau_t}. \tag{132}$$

The signal from inhomogeneities with such dimensions and "true contrast"

$$m_0 = (\sigma_0 - \overline{\sigma_0})/\overline{\sigma_0} \tag{133}$$

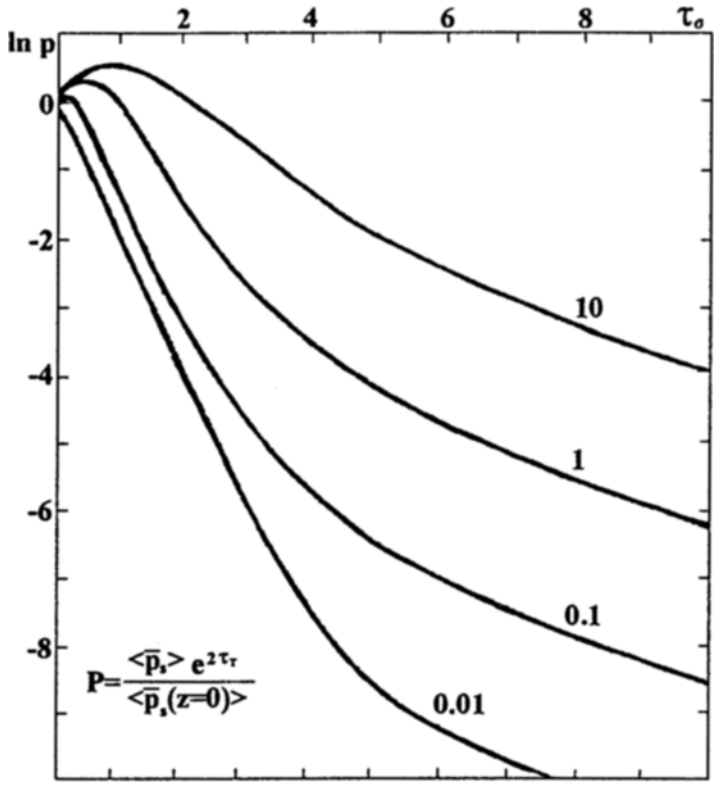

Fig. 5. Signal-power transfer coefficient $\langle \overline{pS} \rangle$ divided by $\langle \overline{pS}(z=0) \rangle \times \exp(-2\tau_t)$ as a function of $\tau_\sigma = \sigma_1 z_0$. The numbers denote the values of the parameter C. The maxima on the curves show the backscattering enhancement.

is distinguished against the background of shot noises of the receiver under the condition (see Eq. (38))

$$m_0 \langle \overline{pS} \rangle \geq \beta(1+\delta)(\mathrm{S/N})_0/\chi, \tag{134}$$

where $(\mathrm{S/N})_0$ is the threshold signal-to-noise ratio. In this case, the visibility range (z_0) is determined from the equation

$$z_0 e^{\frac{2}{3}(\sigma_t+\kappa)z_0} = \left[\frac{m_0\lambda_0^2(c\tau_c/2)\chi}{\langle\cos\gamma\rangle\beta(1+\delta)(\mathrm{S/N})_0}\right]^{1/3}, \tag{135}$$

from which it follows that for the parameter values shown in the above example and under the conditions $(\mathrm{S/N})_0 = 5$, $\delta \ll 1$, $m_0/\langle\cos\gamma\rangle = 0.5$, $\eta P_0 = 50$ μA, and $f_1 = \beta f_0 = 1.5 \cdot 10^5$ Hz ($\beta = 5.4 \cdot 10^{-10}$, $z_c = 1.5$ mm, and $t_c = 0.025$ sec) the distance is $z_0 = 1.16$ mm.

We note that in the general case, when estimating the visibility range, along with the internal noises we must allow for the spatial noise generated by the fluctuations of the useful signal itself (speckle noise). Its correlation scales coincide with the dimensions of the decomposition element (one of them is the line width, and the other is $c\tau_c/2$). Therefore, the useful-signal fluctuations do not prevent us from observation of inhomogeneities σ_0 with sufficiently high contrast m_0, if the inhomogeneity image contains a large number of elements. However, the visibility of local scatterers and weak-contrast large-scale inhomogeneities is restricted exactly by speckle noise. Their visibility can be estimated by standard methods on the basis of the data on the signal-fluctuation statistics and characteristics of the statistically average image.

11. CONCLUSIONS

Having compared the OCT and laser-pulsed vision methods, we conclude that although they use different ways of forming the resolution element with respect to distance, this difference has no impact on the informative properties of the image. An analog of the OCT system is an equivalent pulsed system.

In accordance with the equivalence principle, the turbid-medium tomograms formed by the OCT system with linear amplifier and quadratic detector of a videosignal can be described directly by the theory of pulsed vision based on the image transfer equation and such notions as the function of point blurring and frequency-contrast characteristic. The structures of tomograms obtained in the case of quadratic and linear detection of a videosignal are related by a simple universal relationship. In both cases, the tomogram bears information on the space variations of the backscattering coefficient of the medium.

Thanks to the single-mode regime of radiation and reception of signals and the regular nature of the time structure of a videosignal that forms an image of a point object, the turbid-medium tomograms have the same speckle noise as in holographic images and show coherent backscattering. The useful effect is an increase (by 3 dB) in the intensity of a signal that arrives from the medium from large optical depths. The negative effect is an increase in fluctuations of the image brightness and violation of the monotonic character of the dependence of the average brightness on the depth in the image of the subsurface layer of the medium (which is not related to stratification of its optical properties).

Similar phenomena will appear due to the scattering of light from the boundary irregularities of the medium. To estimate them, we can use the results of the theory of optical observation through a wavy sea surface [20, 21].

In the OCT system with heterodyne photoreceiver, the radiation-source energy is used less efficiently than in the pulsed detection with direct photodetection of the signal. However, in the femtosecond tomography of biological tissues, the visibility depth of their structure is mainly restricted by resolution losses rather than by energy losses.

In particular calculations and estimations we used the simplest (therefore, roughest) models of the light fields. A more universal and rigorous description of tomograms can be developed on the basis of Eqs. (103) – (106), which also allow us to study the possibilities of reconstruction of optical properties of a stratified medium from its images and analyze the possibilities of correction of image distortions related to the inhomogeneity of optical characteristics of the medium on the propagation path of the sounding and backscattered signals. Equations (121c) and (111a) can be used directly to eliminate the error in the determination of the distance to the scatterer that is caused by the photon spread over the paths.

I would like to thank A. V. Gaponov-Grekhov for his interest in this work, A. M. Sergeyev, I. A. Andronova, F. I. Fel'dshtein, V. M. Gelikonov, G. V. Gelikonov, R. V. Kuranov, and D. V. Shabanov for information I acquired during a discussion of OCT problems, V. A. Savel'yev for assistance with the calculations and preparation of the manuscript, and A. G. Luchinin for useful remarks made when reading the manuscript.

This work was supported by the Russian Foundation for Basic Research (project Nos. 95–02-05797 and 96–02–05990) and the Foundation of Leading Scientific Schools (grant No. 96–15– 96592).

REFERENCES

1. V. V. Tuchin, *Usp. Fiz. Nauk*, **165**, No. 5, 517 (1997).
2. D. Huang, J. Wang, C. P. Lin, J. S. Schuman, W. G. Stincon, W. Chang, M. R. Hee, T. Flotte, K. Gregory, C. A. Puliafito, and J. G. Fujimoto, *Science*, **254**, 1178 (1991).
3. V. M. Gelikonov, G. V. Gelikonov, N. D. Gladkova, R. V. Kuranov, N. K. Nikulin, G. A. Petrova, V. V. Pochinko, K. I. Pravdenko, A. M. Sergeev, F. I. Fel'dshteyn, Ya. I. Khanin, and D. V. Shabanov, *Pis'ma Zh. Eksp. Teor. Fiz.*, **61**, No. 2, 149 (1995).

4. A. M. Sergeev, V. M. Gelikonov, G. V. Gelikonov, F. I. Fel'dshtein, N. D. Gladkova, and V. A. Kamenskii, *OSA TOPS Adv. Opt. Imag. Photon Migr., Issue 2*, 196 (1996).

5. A. M. Sergeev, V. M. Gelikonov, G. V. Gelikonov, F. I. Fel'dshtein, R. V. Kuranov, N. D. Gladkova, N. M. Shakhova, L. B. Snopova, A. V. Shakhov, I. A. Kuznetzova, A. N. Denisenko, V. V. Pochinko, Yu. P. Chumakov, and O. S. Strel'tsova, *Opt. Expr.*, 1997.

6. E. P. Zege, A. P. Ivanov, and I. L. Katsev, *Image Transfer in a Scattering Medium* [in Russian], Nauka i Tekhnika, Minsk (1985).

7. Y. Pan, R. Birngruber, J. Rosperich, and R. Engelhardt, *Appl. Opt.*, **34**, No. 28, 6564 (1995).

8. A. Knuttel, R. Schork, and D. Bocker, *Proc. SPIE*, **2655**, 258 (1996).

9. L. S. Dolin and I. M. Levin, *Reference Book in the Theory of Underwater Vision* [in Russian], Gidrometeoizdat, Leningrad (1991).

10. R. V. Kuranov, *Optical Coherence Tomography of Biological Tissues*, Graduation Work, State University, Adv. School Gen. Appl. Phys., Nizhny Novgorod (1995).

11. I. S. Gonorovskii, *Radio Engineering Circuits and Signals* [in Russian], Sovet-skoe Radio, Moscow (1971).

12. A. Ishimaru, *Propagation and Scattering of Waves in Randomly Inhomogeneous Media* [Russian translation], Mir, Moscow (1981).

13. Yu. A. Kravtsov and A. I. Saichev, *Usp. Fiz. Nauk*, **137**, No. 3, 501 (1982).

14. S./ts M. Rytov, Yu. A. Kravtsov, and V. I. Tatarskii, *Introduction to Statistical Radiophysics. Part 2. Random Fields* [in Russian], Nauka, Moscow (1978).

15. L. S. Dolin and V. A. Savel'yev, *Izv. Vyssh. Uchebn. Zaved., Radiofiz.*, **22**, No. 11, 1310 (1979).

16. H. Bremmer, *Radio Sci.*, **68D**, No. 2, 967 (1964).

17. L. S. Dolin, *Dokl. Akad. Nauk SSSR*, **260**, No. 6, 1344 (1981).

18. L. S. Dolin, *Izv. Vyssh. Uchebn. Zaved., Radiofiz.*, **26**, No. 3, 300 (1983).

19. W. F. Cheong, S. A. Prahl, and A. J. Welch, *IEEE J. Quant. Electr.*, **26**, No. 12, 2166 (1990).

20. A. G. Luchinin, *Izv. Akad. Nauk SSSR, Fiz. Atmos. Okeana*, **15**, No. 7, 770 (1979).

21. V. L. Veber and I. A. Sergievskaya, *Izv. Ross. Akad. Nauk, Fiz. Atmos. Okeana*, **28**, No. 3, 325 (1992).